

Dark resonances as a probe for the motional state of a single ion

C. Lisowski, M. Knoop,* C. Champenois, G. Hagel, M. Vedel, and F. Vedel

Physique des Interactions Ioniques et Moléculaires (CNRS UMR 6633),

Université de Provence, Centre de Saint Jérôme, Case C21, 13397 Marseille Cedex 20, France

(Dated: Received: November 11, 2019/ Revised version: date)

Single, rf-trapped ions find various applications ranging from metrology to quantum computation. High-resolution interrogation of an extremely weak transition under best observation conditions requires an ion almost at rest. To avoid line-broadening effects such as the second order Doppler effect or rf heating in the absence of laser cooling, excess micromotion has to be eliminated as far as possible. In this work the motional state of a confined three-level ion is probed, taking advantage of the high sensitivity of observed dark resonances to the trapped ion's velocity. The control of the excess micromotion is tested by monitoring the dark resonance contrast with varying laser beam geometry. The influence of different parameters such as laser linewidth and power has been investigated experimentally and numerically.

PACS numbers: 32.80.Pj, 39.30.+w

I. INTRODUCTION

Dark resonances in a three-level system are a well-known example of destructive quantum interferences based on the interaction of two light fields generating the coherent superposition of two atomic states. Various applications of the coherent population trapping scheme can be found in atomic physics from high-resolution spectroscopy to sub-recoil laser-cooling of an atom cloud [1] or EIT-cooling of single ions [2, 3]. Dark resonances have been readily observed in trapped ions, almost exclusively with copropagating laser beams [4, 5, 6, 7]. In general the observed splitting of the various Zeeman levels is used for an exact quantitative calibration of the local magnetic field.

Single ions confined in radiofrequency traps are ideal candidates for different applications of high-resolution spectroscopy such as quantum information or frequency standards in the optical domain [8]. They can be stored in the trap from hours up to months in a quasi interaction-free environment. Laser cooling of the single trapped ion allows to reach the Doppler cooling limit which is in the mK-range. To eliminate residual Doppler broadening on a given transition by accessing the Lamb-Dicke regime [9], the ion's excursion along the laser propagation direction must be smaller than the inverse wavenumber. The fluorescence spectrum is then decomposed in a central carrier and few sidebands separated by the ion's motional frequencies. This excellent spatial localisation can only be achieved in the low-field region of the rf trapping field confining the ion, corresponding in the majority of cases to the center of the trap. For this purpose, the pseudo-potential at the position of the ion has to be nearly perfectly symmetric. Parasitic potentials due to asymmetries or ion creation may distort the created potential and deviate the minimum of the trap's AC electric field from the minimum of the pseudo-potential well, causing excess micromotion in the ion motion. They have therefore to be corrected by application of additional direct voltages on supplementary correction electrodes in all three directions.

Different experimental techniques have been employed to reduce the excess micromotion of a single trapped ion ([10] and references therein). In this paper we present an additional and straightforward method for the localisation of an ion in the miniature trap. We have used coherent population trapping as a tool to minimize the micromotion of the confined ion. Dark resonances depend ideally only on the lifetimes of the initial and the final state, which in the presented experiment are both very long-lived. In practice, the visibility of the dark resonance is modified by the linewidth and the power of the applied lasers, these experimental parameters can be very well controlled. The main factor of residual broadening of the observed non-absorbing state is then the velocity distribution of the confined ion. The study of the phenomenon reveals that the maximum sensitivity to the kinetic energy state is reached with counterpropagating laser beams. The proposed technique is based on the fact that the contrast of dark resonances observed in a single ion fluorescence increases with the degree of immobilisation of the ion. Actually, excess micromotion "fills" the dip of the dark resonance in the case where the laser beams are counterpropagating.

We trap singly-ionized calcium in a miniature cylindrical radiofrequency trap. The main laser-cooling transition connects the $4S_{1/2}$ ground state to the $4P_{1/2}$ -level at 397 nm. Throughout the manuscript this is called the blue

*Electronic address: Martina.Knoop@up.univ-mrs.fr

transition (index B). This upper state has a lifetime of 7 ns and a branching ratio to the metastable $3D_{3/2}$ -state of about 6%. A closed laser-cooling cycle therefore requires a repumper laser at 866 nm (red transition (R)) to empty the $3D_{3/2}$ -state. The observed dark resonances are the sign of the coherent superposition of the $4S_{1/2}$ ground state and the metastable $3D_{3/2}$ -state which has a lifetime of about one second [11, 12]. The level-scheme of the Ca^+ -ion dressed by the blue photons is given in the inset of Figure 1.

Our experimental set-up uses a miniature ring trap with an inner diameter of 1.4 mm. The trapping frequency of $\Omega/2\pi \simeq 12$ MHz with an amplitude of about $V_{AC} = 300$ V is applied to the ring, generating a pseudo-potential well with a depth of a few eV , allowing the confinement of ions for very long periods. Two tip electrodes in the plane of the ring (x, y) and two larger mesh electrodes along the ring axis (z_1, z_2), distant by approximately 5 mm from the ring center, permit corrections of the potential by application of direct voltages. The trapping characteristics of this device are described in detail elsewhere [13].

The first section of this article describes the micromotion generated in the radiofrequency trap, the existing methods to reduce this effect are very briefly reviewed. We then introduce the formalism for dark resonances, along with the modeling used to obtain a high degree of control of the experimental conditions. The last section of this work is devoted to the experimental and numerical observation of dark resonances. The influence of the main control parameters (laser power, beam geometry and magnetic field) are discussed.

II. MICROMOTION IN A PAUL TRAP

The motion of a trapped ion in an ideal Paul trap is described by the Mathieu equations [14]:

$$\frac{d^2u}{d\tau^2} + [a_u - 2q_u \cos(2\tau)]u = 0 \quad \text{with} \quad \tau = \frac{\Omega}{2}t \quad (1)$$

valid for the three directions $u = x, y, z$. The values of the coefficients a_u and q_u which determine the range of stable confinement of a particle are defined by the trapping voltage V_{AC} and its frequency $\Omega/2\pi$, the superimposed DC-voltage V_{DC} , the radius r_0 of the trap as well as the e/m ratio of the trapped ion. To first order in a_u and q_u , the stable solution of equation (1) is

$$u(t) = R_u \cos \omega_u t \left(1 + \frac{q_u}{2} \cos \Omega t\right) \quad (2)$$

The motion of the confined ion is composed of the harmonic oscillation at frequencies $\omega_u/2\pi$ with amplitude R_u called "secular" motion, and the AC-driven "micromotion" at the frequency of the trapping field $\Omega/2\pi$. In opposition to the secular motion, micromotion cannot be cooled because it is driven motion. According to Eq.(2), a smaller secular motion amplitude R_u leads to a reduced contribution of the micromotion. A displacement of the ion from the center of the trap due to asymmetries in the geometry of the trap and the applied electric fields, may cause excess micromotion, which can possibly prevent the access to the Lamb-Dicke regime. A complete review of origin and consequences of the micromotion is given in [10].

Three experimental methods allow to control excess micromotion of an ion in a radiofrequency trap. Best results are obtained by using all of them as the collected information is complementary in the three cases. The control parameter is in either case the set of DC-voltages applied to the four (x, y, z_1, z_2) compensation electrodes surrounding the trap. The most simple approach is the observation of the spatial displacement of a trapped ion as the confining potential is lowered. Parasite potentials then gain in importance and move the ion out of the trap center. This method requires spatial detection of the ion's fluorescence and is limited to the plane of observation. Another means for the rejection of excess micromotion is to probe the fluorescence linewidth of the laser-cooling transition. This profile is difficult to calibrate in terms of absolute temperature, but gives a good relative control signal of the ion's kinetic energy when laser powers are fixed. At a given laser frequency, the half-maximum fluorescence signal decreases for better compensation, as the ion becomes colder and its blue transition linewidth narrower. A more specific observation of the micromotion's influence is the measure of the correlation of the emitted fluorescence photons with the confinement frequency $\Omega/2\pi$ [10]. Actually, the oscillatory motion of the ion causes a frequency modulation of the laser field in the rest frame of the ion, and induces a modulation of the emitted photons at the trapping frequency $\Omega/2\pi$. To cancel the micromotion, the amplitude of this modulation signal has to be minimized. Best compensation results are obtained by the use of different laser axes for an access to the different projections in space.

The ultime measurement to determine the absolute degree of localisation of the ion in the trap is the detection of vibrational sidebands. The oscillatory motion at a fixed frequency leads necessarily to sidebands, in the case of the trapped ions at the trapping frequency $\Omega/2\pi$ and the secular frequencies $\omega_u/2\pi$. The relative height of the sidebands is related to the amplitude of the corresponding oscillation, and their minimization is thus an indicator for

the localization of the ion [15]. Sideband observation is only possible on a transition whose natural linewidth is inferior to the ion's vibrational frequencies. In our case, it must be realized on the ultra-narrow $4S_{1/2} - 3D_{5/2}$ transition using the quantum jump technique. The experimental realization requires a highly stabilized laser to excite the $4S - 3D$ transition and the need to work on quantum jump statistics for the detection of this dipole-forbidden transition.

In the following we will show how we can use the varying-contrast observation of the coherent population trapping dip as a probe for the minimisation of the micromotion of the confined particle.

III. FORMALISM AND MODELING

In a three-level system driven by two lasers, coherent superposition of the atomic states coupled by the radiation fields may lead to the appearance of a non-absorbing state, when the detunings of the cooling laser (B) and the repumper (R) are equal. In this case, one of the stationary states $|\psi_{NC}\rangle$ of the atomic system in the Λ configuration undergoing excitation by two lasers, is a coherent superposition of the ground and metastable states $S_{1/2}$ and $D_{3/2}$, which is not coupled to the excited state $P_{1/2}$ by the atom-laser interaction V_L ($\langle P_{1/2} | V_L | \psi_{NC} \rangle = 0$). Once in this state, the atom can not absorb or scatter photons and the fluorescence disappears. This feature, called dark resonance, has been used to cool atoms below the recoil limit by velocity selective coherent population trapping [16], and for other applications detailed in [1].

In the general case, the two transitions are driven by different lasers, the non-coupled state then depends on the relative phase of the lasers like:

$$|\psi_{NC}\rangle = e^{-i(\omega_B t + \phi_B)} \frac{-\Omega_B |D_{3/2}\rangle + \Omega_R e^{-i((\omega_R - \omega_B)t + \phi_R - \phi_B)} |S_{1/2}\rangle}{\bar{\Omega}} \quad (3)$$

with $\bar{\Omega} = \sqrt{\Omega_B^2 + \Omega_R^2}$, where we suppose the two Rabi pulsations Ω_B and Ω_R , on the blue and red transitions, to be real. This dependance implies a high stability of the applied lasers to observe the complete extinction of the emitted fluorescence.

If the progressive wave nature of the laser fields and the kinetic energy of the atom are taken into account, the laser couples $|P_{1/2}, p\rangle$ with $|S_{1/2}, p - \hbar k_B\rangle$ and $|D_{3/2}, p - \hbar k_R\rangle$, where p , $\hbar k_B$ and $\hbar k_R$ are respectively the projection of the atom momentum, a blue and a red photon momentum, along the common propagation axis of the two lasers. Then, the non coupled state is not an eigenstate of the kinetic energy and is coupled to its orthogonal state $|\psi_C\rangle$ by the kinetic energy operator:

$$|\psi_C\rangle = \frac{\Omega_R e^{-i(\omega_R t + \phi_R)} |D_{3/2}, p - \hbar k_R\rangle + \Omega_B e^{-i(\omega_B t + \phi_B)} |S_{1/2}, p - \hbar k_B\rangle}{\bar{\Omega}} \quad (4)$$

In the basis of the atom dressed by N_B blue photons and N_R red photons, we study the evolution of the system inside the family state \mathcal{F}_p defined by p

$$\mathcal{F}_p = \{ |S_{1/2}, p - \hbar k_B, N_B + 1, N_R\rangle; |P_{1/2}, p, N_B, N_R\rangle; |D_{3/2}, p - \hbar k_R, N_B, N_R + 1\rangle \} \quad (5)$$

The non-coupled state is coupled to its orthogonal state by

$$\langle \psi_C | H_0 + \frac{p^2}{2m} + V_L | \psi_{NC} \rangle = \langle \psi_C | H_0 + \frac{p^2}{2m} | \psi_{NC} \rangle = \frac{\Omega_B \Omega_R}{\bar{\Omega}^2} \left(\hbar(\Delta'_B - \Delta'_R) + p \frac{\hbar(k_R - k_B)}{m} \right) \quad (6)$$

where Δ'_R and Δ'_B are the laser detunings corrected by the photon recoil energy: $\Delta' = \omega - \omega_{at} + \hbar^2 k^2 / 2m$. In the case of two identical-wavelength transitions driven by copropagating laser beams ($k_R = k_B$), the non coupled state is stationary as soon as the corrected detunings are equal. If the two laser beams are counterpropagating or in the more general case of different wavelengths ($|k_R| \neq |k_B|$), the non-coupled state is stationary only if the atom is at rest in the excited state ($p = 0$). $(-\Omega_B |D_{3/2}, -\hbar k_R\rangle + \Omega_R |S_{1/2}, -\hbar k_B\rangle) / \bar{\Omega}$ is then a perfect trap state, as long as we neglect its finite lifetime caused by spontaneous emission. In the case of a moving atom, the dark resonance condition can be interpreted as an equality of the two detunings corrected by the Doppler shift :

$$\Delta'_B - k_B p/m = \Delta'_R - k_R p/m \quad (7)$$

It appears from the above equation that the observation of the dark resonances can be used to quantify the motional state of an ion, and that the highest sensitivity to this motion is obtained for $k_R = -k_B$.

To identify the dependance of the dark resonance profile of each experimental parameter (laser linewidth, laser intensity and detuning, motional state of the ion), we numerically studied the atomic system through the evolution of

its density matrix. The dark resonances are visualized by calculating the population of the $4P_{1/2}$ -level as a function of the red laser detuning. The theoretical and numerical studies regarding VSCPT and cooling below the recoil limit [17] on a symmetric Λ system showed that the full treatment implies the discretisation of the momentum space. This method requires very long computational time and is not needed for the precision demanded here. Because the frequency resolution and the natural linewidths of the transitions are in the MHz-range, far above the photon recoil shift, and because the mechanical effect of light is omitted, we may neglect the operators due to the kinetic energy of the ion in the density matrix. Using the same approach as in [18], we add the Doppler shift in the laser detuning like in equation (7). The detunings are then oscillating with the ion in the trap with a velocity deduced from Eq. (2). For the sake of simplicity, we suppose here that only one secular frequency (ω_r) contributes to the Doppler shift:

$$\Delta(t) = \omega_L - \omega_{at} \pm k \left(V_0 \sin \omega_r t \left(1 + \frac{q_r}{2} \cos \Omega t \right) + \sqrt{2} V_0 \cos \omega_r t \sin \Omega t + \frac{a}{R_r} V_0 \sqrt{2} \sin \Omega t \right) \quad (8)$$

where the sign of the Doppler shift is defined by the propagation direction of the laser. The displacement a of the average position of the ion relative to the oscillation amplitude R_r gives rise to excess micromotion. As the natural widths of the involved atomic transitions are of the same order as the secular oscillation frequency ($\Gamma_B/2\pi = 20.6$ MHz, $\Gamma_R/2\pi = 1.7$ MHz, $\omega_r \simeq 1$ MHz), the ion can not be considered as free and the oscillatory motion of the ion has to be followed during several periods, until convergence is reached. The laser linewidths Γ_{LB} and Γ_{LR} (FWHM) are taken into account by a relaxation on coherence. To prevent pumping in a dark state, a minimal magnetic field must be applied and several dark resonances can be observed, corresponding to the different Zeeman sub-levels. The density matrix is solved for the eight Zeeman sublevels of the $S_{1/2}, P_{1/2}, D_{3/2}$ system.

IV. RESULTS

The experimental setup is like in [19] and in figure 1, where the case of counterpropagating laser beams is depicted. The ultrahigh-vacuum vessel containing the miniature trap allows the propagation of the laser beams along an axis having a 55 degree angle according to the trap's z -axis. Observation of the ion's fluorescence is made in the xy -plane of the trap either spatially resolved by an intensified CCD or as an integrated signal by a photomultiplier in photon-counting mode. Laser beams are transported to the trap by single-mode fibers, polarization-maintaining in the case of the blue laser. Laser polarizations are modified by means of quarter- and half-waveplates.

Dark resonances require identical detuning for both lasers, their observation can be readily realized by keeping one laser fixed, while probing the atomic resonance with the other laser. To avoid the influence of varying laser-cooling, we fix the blue cooling laser on the red-frequency side of the $4S_{1/2}$ - $4P_{1/2}$ transition (approximately at -1 to $-2 \Gamma_B$) and scan the frequency of the repumper laser at 866 nm. We define the "contrast" \mathcal{C} of the dark resonance at a given frequency as the depth of the observed dip divided by the possible total signal if we suppose a roughly Gaussian lineshape.

To illustrate the numerical approach described in the preceding section, figure 2 shows the variation of the observed dark resonance as a function of the displacement a from the trap center which gives rise to excess micromotion. This simulation has been carried out with counterpropagating laser beam geometry. Parameters for the simulations are chosen corresponding to the observed experimental spectra (laser linewidths $\Gamma_{LB} = 1$ MHz and $\Gamma_{LR} = 0.2$ MHz, magnetic field $B = 1$ G, and Rabi pulsations $\Omega_B = 120$ MHz and $\Omega_R = 30$ MHz). The secular frequency has been taken to be $\omega_r/2\pi = 1$ MHz and the ion's velocity fixed to $v_0 = 5$ m/s which corresponds to a temperature of 0.14 K. The lower curve in figure 2 has been computed with a displacement from the trap center equal to the amplitude of oscillation $R_r = 0.8 \mu\text{m}$, and the upper curve with $2R_r$. For these parameters, the linewidth of the blue $4S_{1/2} - 4P_{1/2}$ cooling and detection transition is approximately 11% larger for the upper curve than for the lower curve.

A. Magnetic field

To make sure that laser polarization effects do not play a role, the local magnetic field has to be controlled in a rigorous way. We apply a magnetic field sufficient to define a quantization axis but small enough to avoid the splitting of the Zeeman sublevels. In our experimental setup, the local magnetic field is controlled by three pairs of orthogonal Helmholtz coils. The residual \vec{B} -field at the position of the ion has been compensated making use of the Hanle effect. Laser-cooling is carried out on the $4S_{1/2} - 4P_{1/2}$ transition, while a repumper on the $3D_{3/2} - 4P_{1/2}$ transition at 866 nm avoids trapping of the ion in the metastable $3D_{3/2}$ state. A bias magnetic field \vec{B}_0 (≈ 1 Gauss) is applied perpendicularly to the propagation axis of the lasers, the repumping laser being linearly polarized parallel to this field. If the total magnetic field is parallel to \vec{B}_0 , the ion is pumped in the $3D_{3/2}$, $m_F = \pm 3/2$ states, which

are not coupled to the laser, making the fluorescence disappear. Any residual magnetic field perpendicular to \vec{B}_0 mixes these dark states with the $3D_{3/2}$, $m_F = \pm 1/2$ states and fluorescence is then observed again. If the repumping laser polarisation is purely linear, the observed fluorescence can be reduced to zero when the applied magnetic field exactly compensates the local field (see figure 3). This procedure is carried out for all three axis of the magnetic field, changing the quantization axis and the corresponding laser polarizations. The method, based on optical pumping in a dark state, is independent on the linewidth and detuning of the lasers, if we assume that the bias magnetic field is small enough to keep the splitting of the Zeeman sublevels comparable to the excitation linewidth of the lasers. As a consequence, this technique is not sensitive to the motion of the ion and presents the advantage of being useable for a single ion as well as for an ion cloud.

B. Laser intensity

The observed dark resonances are explained in the frame of the atom dressed by the blue photons (see inset in figure 1). The width of the $S_{1/2}$ and the $P_{1/2}$ dressed states and the splitting between the levels depend on the laser intensity and detuning (light shift), in contrast to the frequency position of the dark resonance that separates them. In particular, higher laser intensity at 397 nm splits the atomic levels to a greater extent and increases the visibility of the dark resonance. The five graphs in figure 4 have been taken with increasing laser power, starting from 20 μW which corresponds to a Rabi frequency of 15 Γ_B . The digging of the dark resonance dip with the applied blue laser power follows a saturation curve as represented in the inset of the figure. For laser intensities higher than 30 Γ_B the transition is largely saturated, and the maximum visibility of the dark resonance is reached.

We have also checked the influence of the red probe laser intensity while keeping the blue laser power fixed. As expected, this only broadens the scanned atomic transition, without increasing the visibility of the dark resonance, as power broadening effects prevail on the light shift effect.

C. Micromotion

For counterpropagating laser beams, dark resonances have merely be observed in our experiment when the ion is well localized, which means that part of the excess micromotion has already been eliminated by a rough compensation of patch potentials. Actually, simulations show the dependence of the contrast of the dark resonance on the degree of localisation of the ion (see figure 2). The smaller the ion's amplitude of motion, the deeper the observed dark resonance. In figure 5 several graphs show the changing contrast in the observation of a dark resonance, as a function of modified compensation voltages applied on the correction electrodes. We have made sure, that the additional static voltages do not push the ion out of the laser beams. The inset shows the contrast \mathcal{C} of the dark resonance versus the applied compensation voltage and a maximum can be unambiguously distinguished. We have verified that this maximum corresponds to a reduced spectral linewidth of the blue cooling transition. The blue linewidth represents an estimate of the ion's kinetic energy when approximated by a Doppler profile. It cannot be taken as an absolute measure as it depends strongly on the applied (blue) laser intensity, however it is a good relative indication of the kinetic energy state of the ion. Compensation parameters have been tested on all four correction electrodes, resulting in the best localisation of a single ion.

D. Laser beam geometry

We have used the observed dark resonances to collect information about the motional state of the ion using equation (7). If we take into account experimental parameters as the laser power or spectral width, the collapse of the fluorescence due to a dark resonance is observable for relative detunings $\Delta'_B - \Delta'_R \leq \delta$. The dark resonance condition is then fulfilled for a velocity class δv , which is inversely proportional to the difference or the sum of the wavenumbers depending on the laser beam geometry:

$$\delta v_{\uparrow\uparrow} = \frac{\delta}{k_B - k_R} \quad (9a)$$

$$\delta v_{\uparrow\downarrow} = \frac{\delta}{k_B + k_R} \quad (9b)$$

where a) denotes the case of copropagating laser beams, while b) stands for counterpropagating laser beams.

In the case of a Ca^+ ion $k_B \approx 2k_R$, which means that the velocity class participating in the dark resonance in the copropagating laser beam configuration is three times larger than in the case of counterpropagating laser beams. For a laser-cooled ion oscillating in the trap and with observation times which are at least two orders of magnitude higher than the oscillation timescale, the observed signal is smeared out in the case of counterpropagating laser beams leading to a lower contrast as can be seen on the computed graphs in figure 6.

The geometry of counterpropagating cooling laser beams in our experiment allows to use the contrast of the observed dark resonances as a tool for the minimization of the micromotion. We have also worked with the alternative beam geometry where both lasers enter the trap from the same direction. In this configuration, dark resonances can be observed in almost any case, even with a small ion cloud. As example, figure 7 shows the fluorescence spectrum of three ions with copropagating laser beams. To evidence the difference between co- and counterpropagating laser beam geometry we have plotted the dark resonance contrast \mathcal{C} as a function of the experimental linewidth of the $4S_{1/2} - 4P_{1/2}$ transition in figure 8. Again, the blue transition linewidth gives a relative indication of the degree of localisation of the trapped ion, as the smaller it is, the closer the ion is to the center of the trap. The dispersion of the points in figure 8 is due to slightly different levels of probe and cooling laser intensity. Nevertheless the general tendency is clearly visible: while dark resonances could not be observed at all for the counterpropagating geometry unless a certain level of localization has been reached, the copropagating geometry allows the observation of dark resonances for much hotter ions and even for small ion clouds. We have been able to deepen the dark resonance dips for both geometries almost down the background light level, reflecting an excellent localisation of the ion. The counterpropagating laser beam geometry seems to be able to reveal the degree of localization of the trapped ions with a greater sensitivity.

V. CONCLUSION

In this paper we have presented a novel approach to reduce the micromotion of an ion confined in a miniature electrodynamic trap. We use the contrast of the dark resonances observed with two counterpropagating laser beams to collect information about the motional state of the ion. Numerical simulations and experiments have shown that this contrast is very sensitive to the localisation of the ion, while a larger micromotion amplitude smears out the coherent population trapping effect. Observation of fluorescence is made on time bins which are long compared to the inverse motional frequencies of the ion. On this timescale, the oscillation amplitudes along the three directions are coupled in the trap. Using highly-stabilized lasers, the acquisition of the signal can be made by comparing the fluorescence level at two frequencies (dark resonance minimum and fluorescence signal maximum). Only the lasers for cooling and detection of the ion are necessary for the implementation of the proposed technique, in contrast to other techniques, in particular the probing of the vibrational sidebands which requires a highly stabilized laser to probe a narrow-linewidth transition.

A quantitative comparison with other compensation techniques is not straightforward as the different methods produce various signal levels and use different sets of experimental parameters. In any case, the maximum fluorescence signal has to be monitored as a function of the compensation voltages, to make sure that a decrease in the observed signal height is not due to the fact that the ion has been pushed out of the laser beams. Measurements along multiple laser axes have to be performed to assure a complete extinction of excess micromotion for all projections in space.

The spatial displacement of the confined particle with lowered pseudo-potential well depth requires the use of a detector with spatial resolution and can only be applied to reduce effects which appear in the plane of observation. The exploration of the linewidth on the $4S_{1/2} - 4P_{1/2}$ -transition is an easy method to minimize excess micromotion roughly, keeping in mind that the linewidth depends also on the applied laser intensities and frequencies which may modify the efficiency of laser cooling. Excess micromotion may also deform the excitation spectrum of the ion, it is therefore important to record the entire frequency response at fixed laser intensities. The fluorescence correlation method which shows the modulation of the ion's fluorescence with the micromotion frequency Ω gives best signal-to-noise ratios in the low intensity limit but requires an integration time of at least a couple of seconds to accumulate sufficient signal in each time channel of a time-to-amplitude converter [10].

In summary, we propose a complementary method to reduce excess micromotion of a single trapped ion making use only of the experimental means necessary to detect the ion's fluorescence. In a more general way, this technique can be applied to any three-level ion having a Λ energy scheme, the highest sensitivity being reached for $k_B = k_R$.

[1] E. Arimondo: *Coherent Population Trapping in Laser Spectroscopy*, vol. XXXV (Progress in Optics), E. Wolf (ed.), Elsevier Science 1996.

- [2] C. F. Roos, D. Leibfried, A. Mundt, F. Schmidt-Kaler, J. Eschner, and R. Blatt: Phys. Rev. Lett. **85**, 5547 (2000).
- [3] G. Morigi: Phys. Rev. A **67**, 033402 (2003).
- [4] G. Janik, W. Nagourney, and H. Dehmelt: J. Opt. Soc. Am. B **2**, 1251 (1985).
- [5] Y. Stalgies, I. Siemers, B. Appasamy, T. Altevogt, and P. E. Toschek: Europhys. Lett. **35**, 259 (1996).
- [6] D. Reiss, K. Abich, W. Neuhauser, Ch. Wunderlich, and P.E. Toschek: Phys. Rev. A **65**, 053401 (2002).
- [7] F. Kurth, T. Gudjons, B. Hilbert, T. Reisinger, G. Werth, and A.-M. Maartensson-Pendrill: Z. Phys. D. **34**, 227 (1995).
- [8] Patrick Gill (ed.), *Proceedings of the Sixth Symposium on Frequency Standards and Metrology*: World Scientific Ltd, Singapore 2002.
- [9] R. H. Dicke.: Phys. Rev **89**, 472 (1953).
- [10] D.J. Berkeland, J.D. Miller, J.C. Bergquist, W.M. Itano, and D.J. Wineland: J. Appl. Phys. **83**, 5025 (1998).
- [11] M. Knoop, M. Vedel, and F. Vedel: Phys. Rev. A **52**, 3763 (1995).
- [12] J. Lidberg, A. Al-Khalili, L.-O. Norlin, P. Royen, X. Tordoir, and S. Mannervik: J. Phys. B **32**, 757 (1999).
- [13] C. Champenois, M. Knoop, M. Herbane, M. Houssin, T. Kaing, M. Vedel, and F. Vedel: Eur. Phys. J. D **15**, 105 (2001).
- [14] W. Paul: Rev. Mod. Phys. **62**, 531 (1990).
- [15] F. Diedrich, J.C. Bergquist, W.I. Itano, and D.J. Wineland: Phys. Rev. Lett. **62**, 403 (1989).
- [16] A. Aspect, E. Arimondo, R. Kaiser, N. Vansteenkiste, and C. Cohen-Tannoudji: Phys. Rev. Lett. **61**, 826 (1988).
- [17] A. Aspect, E. Arimondo, R. Kaiser, N. Vansteenkiste, and C. Cohen-Tannoudji: J. Opt. Soc. Am. B **6**, 2112 (1989).
- [18] M. Schubert, I. Siemers, and R. Blatt: Phys. Rev. A **39**, 5098 (1989).
- [19] M. Knoop, C. Champenois, G. Hagel, M. Houssin, C. Lisowski, M. Vedel, and F. Vedel: Eur. Phys. J. D **29**, 163 (2004).

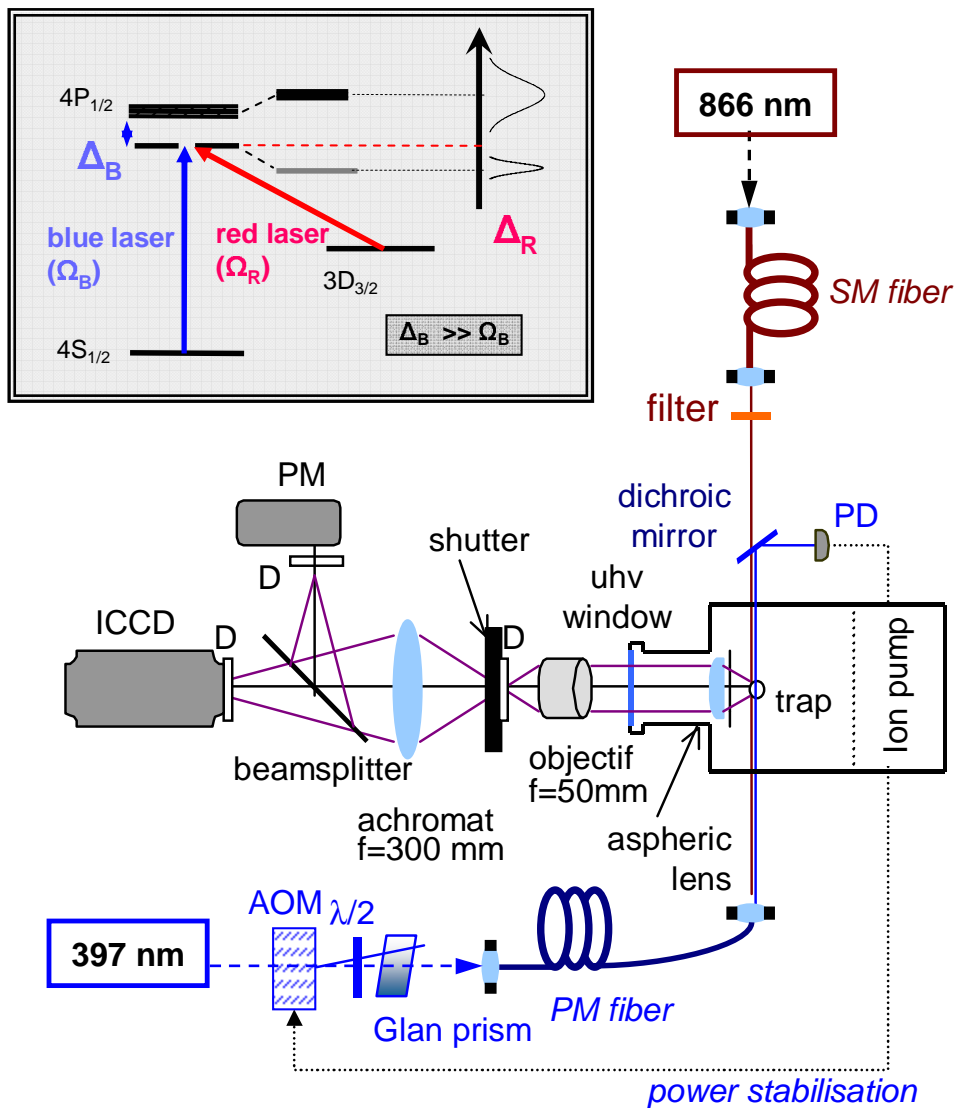


FIG. 1: Experimental setup with counterpropagating laser beams. The left-hand inset shows the first energy levels of a Ca^+ -ion dressed by the blue photons.

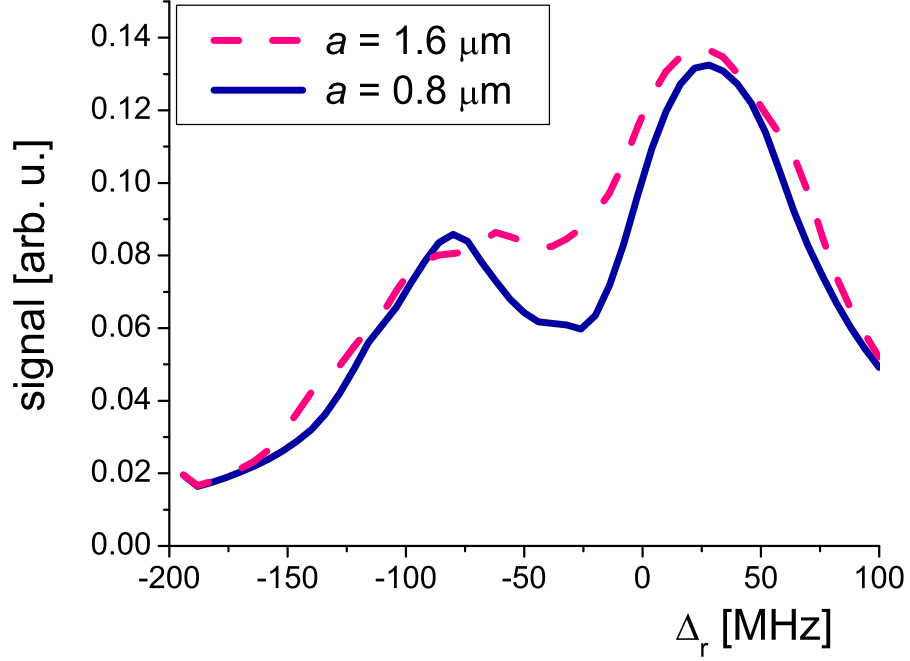


FIG. 2: Calculated fluorescence rate versus the red laser detuning Δ_R for different displacements a from the center of the trap, see detailed explanation in the text.

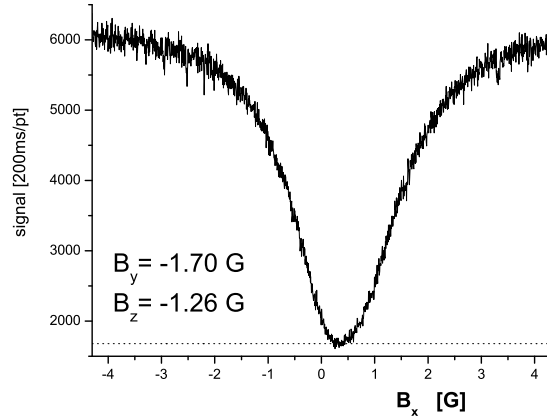


FIG. 3: Fluorescence of a single ion versus the applied perpendicular magnetic field in a Hanle type experiment for the determination of the magnetic field zero values. The red laser is linearly polarized along the x direction. The dotted line corresponds to the background light level.

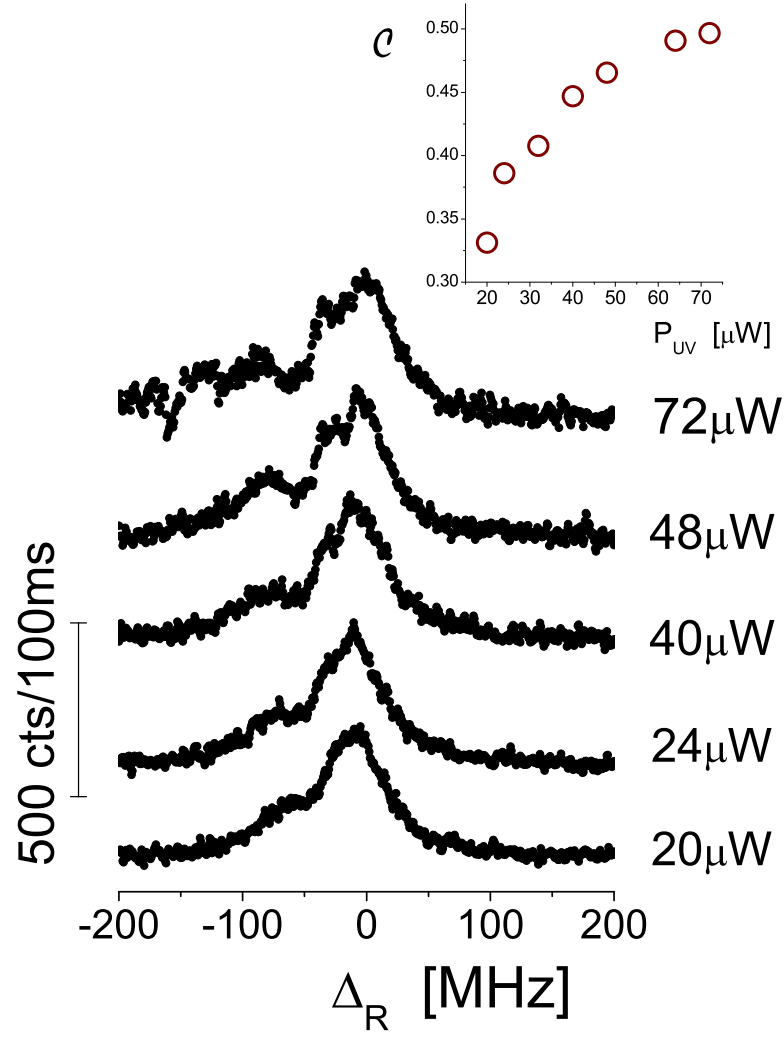


FIG. 4: Dark resonances observed with counterpropagating laser beams. The graph shows the influence of the laser power on the level splitting, the offset of the curves is due to the varying laser power. The applied blue laser powers are marked on the right-hand side of the curves, where the lowest value corresponds to about 15Γ while the highest power is equivalent to 30Γ . The inset shows the increasing contrast of the dark resonance with higher laser power.

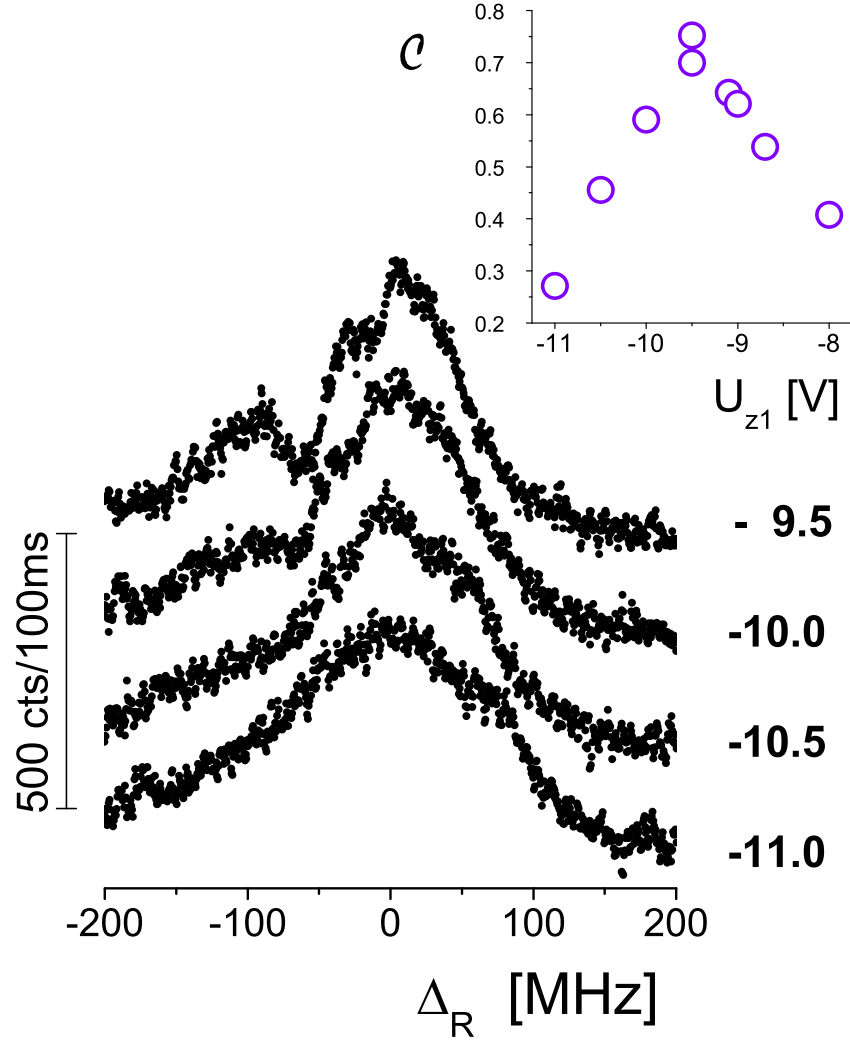


FIG. 5: Influence of the micromotion on the observed dark-resonance contrast C with counterpropagating laser beams, laser intensity: $\Omega_B \approx 30\Gamma_B$, $\Omega_R \approx 100\Gamma_R$. For better visibility, the graph only shows selected curves which have been offset by a fixed value. The compilation of the contrast data in the inset allows an unambiguous determination of the best compensation parameter.

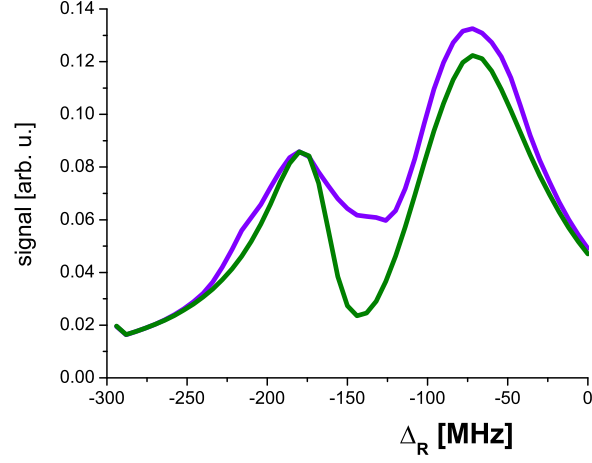


FIG. 6: Simulation of dark resonances with co- and counterpropagating laser beams (lower and upper curve respectively) for an identical amount of micromotion. Excess micromotion reduces the visibility of the dark resonance in the case of the antiparallel laser beam geometry. Parameters are identical to figure 2, $a = 0.8\mu m$.

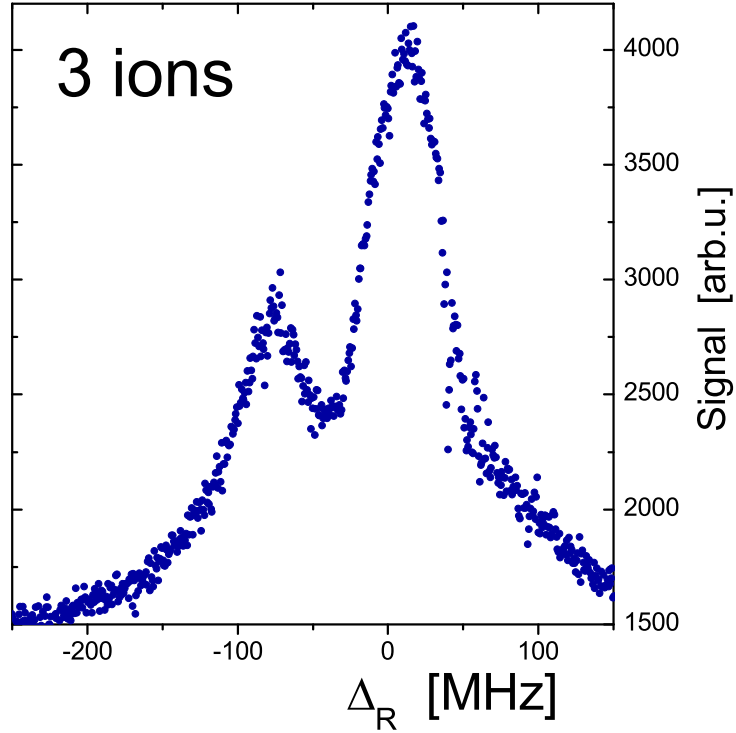


FIG. 7: Dark resonance observed in the fluorescence of a 3-ion cloud with copropagating laser beams.

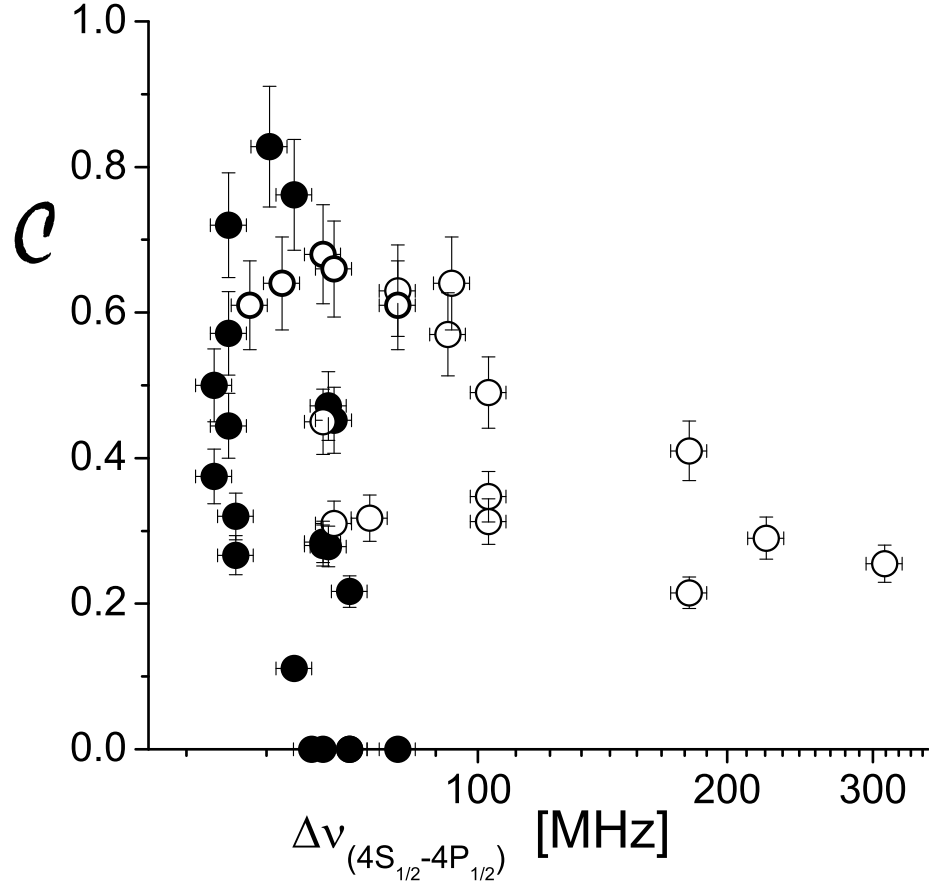


FIG. 8: Comparison of the contrast of the dark resonance for co- (○) and counter-propagating (●) laser beam geometry as a function of the observed transition linewidth on the $4S_{1/2}-4P_{1/2}$ transition. The data for the copropagating geometry has been taken with a single ion below a linewidth of about 100 MHz, and with very small ion clouds (inferior to 10 particles) above.